Andreev edge channels and magnetic focusing in normal-superconductor systems: A semiclassical analysis

P. Rakyta,[1] A. Kormányos,[2] Z. Kaufmann,[1] and J. Cserti[1]
[1]*Department of Physics of Complex Systems, Eötvös University, Pázmány Péter sétány 1/A, H-1117 Budapest, Hungary*
[2]*Department of Physics, Lancaster University, Lancaster LA1 4YB, United Kingdom*
(Received 20 March 2007; revised manuscript received 19 June 2007; published 14 August 2007)

We study a transverse electron-hole focusing effect in a normal-superconductor system. The spectrum of the quasiparticles is calculated both quantum mechanically and in semiclassical approximation, showing an excellent agreement. A semiclassical conductance formula is derived, which takes into account the effect of electronlike as well as holelike quasiparticles. At weak magnetic fields, the semiclassical conductance shows characteristic oscillations due to the Andreev reflection, while for stronger fields it goes to zero. These findings are in line with the results of previous quantum calculations and with the expectations based on the classical dynamics of the quasiparticles.

DOI: 10.1103/PhysRevB.76.064516 PACS number(s): 74.45.+c, 03.65.Sq, 05.60.Gg, 75.47.Jn

I. INTRODUCTION

Investigation of electron-transport properties of normal-superconductor (NS) hybrid nanostructures has attracted considerable experimental[1–6] and theoretical[8–14] interest in recent years. A very important physical process in this respect is the Andreev reflection,[15] whereby an electron incident on a superconductor-normal interface is (partially) retroreflected as a hole into the normal conductor and a Cooper pair is created in the superconductor. The first direct experimental observation of the peculiar property of the Andreev reflection, i.e., that all velocity components are reversed, was achieved by Benistant *et al.*[2,3] using the versatile tool of transverse electron focusing (TEF).[16] The experimental and theoretical investigation of the two-dimensional electron gas using the TEF technique has been pioneered by van Houten *et al.*[17] (see also a recent review[18] discussing these experiments in terms of coherent electron optics).

A particularly interesting problem in NS systems is the interplay of edge channel formation and the Andreev reflection in high magnetic fields.[5–9,13,14] Hoppe *et al.*[8] studied this problem at the interface of semi-infinite superconductor and normal regions in a strong magnetic field parallel to the interface. They found that similarly to the normal quantum-Hall systems, edge states are formed which propagate along the NS interface but these "Andreev" edge states consist of coherent superposition of electron and hole excitations. Therefore, they are a new type of current-carrying edge states which are induced by the superconducting pair potential. The authors of Ref. 8 also showed that a semiclassical approximation can give a good agreement with the exact results obtained by solving the Bogoliubov–de Gennes equation[19] (BdG) for the energy dispersion of the Andreev edge states. Clear experimental evidence for the electron and hole transport in edge states has been reported by Eroms *et al.*[5]

In a disk geometry, it was shown in Refs. 20 and 21 that such edge states can exist both in the presence and also in the absence of any magnetic field and that the bound state energies calculated semiclassically agree very well with the results obtained from the BdG equation.

Giazotto *et al.*[13] have extended the study presented in Ref. 8 by considering the effect of the Zeeman splitting and of the diamagnetic screening currents in the superconductor on the Andreev edge states. Very recently, Fytas *et al.*[11] studied the magnetic field dependence of the transport through a system consisting of a normal billiard and a superconducting island, while Chtchelkatchev and Burmistrov have considered the role of the surface roughness in NS junctions.[14]

In this work, we study the NS hybrid system depicted in Fig. 1. It is similar to the experimental setup of Ref. 2 but in our system the normal conducting region is a two-dimensional electron gas. It is assumed that the quasiparticle transport in the waveguide is ballistic and that the waveguide can act as a drain, which absorbs any quasiparticles exiting to the left of the injector or to the right of the collector.

First, we calculate the eigenstates of this system when the quantum point contacts are not present, i.e., we consider a normal waveguide in contact with a superconductor. We show how the interplay of the lateral confinement brought about by the finite width of the lead, the applied magnetic field, and the proximity effect gives rise to a rich physics in this system. We calculate the eigenstates of the system by solving the BdG equation and then these exact quantum re-

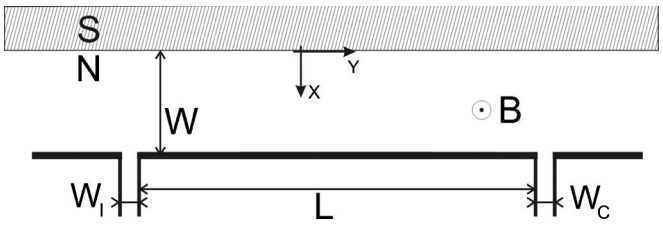

FIG. 1. The hybrid NS nanostructure that we investigate. It consists of an infinitely long two-dimensional ballistic normal conductor of width W coupled to a semi-infinite spin-singlet superconductor region. The conductance is measured between two normal conducting quantum point contacts: the injector (of width W_i) and the collector (of width W_c and at distance L from the injector). The magnetic field B is applied perpendicular to the system (in our calculation, $B>0$ corresponds to a field pointing out of the plane of the system).

sults are compared with results obtained from semiclassical calculations. As we shall show below, the agreement is excellent. We note that the semiclassical approximation we used is applicable in a wider parameter range than the one used in Refs. 8 and 13 for a similar system.

Having obtained the exact eigenstates and their semiclassical approximations, we then turn to the calculation of conductance for the case when the two quantum point contacts, as depicted in Fig. 1, are present. To determine the conductance between the injector and the collector, we adopt the method used by van Houten *et al.*[17] to describe the TEF in a two-dimensional electron gas. In our system, however, we have to take into account the dynamics of both the electronlike and of the holelike quasiparticles. Thus, our results can be considered as a generalization of the corresponding semiclassical calculations of Ref. 17.

Recently, the same NS system has been studied numerically[22] using a Green's function technique.[23] The influence of the underlying classical dynamics on the conductance has been, however, discussed only qualitatively. Our rigorous semiclassical treatment gives a quantitative analysis of the dependence of the transport on the classical dynamics of quasiparticles.

The rest of the paper is organized as follows. In Sec. II, we present the exact quantum calculations based on the BdG equation. Then, in Sec. III, we discuss the results of the semiclassical approximations of the exact quantum calculations. In Sec. IV, we compare the results of the quantum and of the semiclassical calculations and give the physical interpretation of the results. Section V is devoted to the semiclassical calculation of the conductance between the injector and the collector, which is the central result of our paper. Finally, in Sec. VI, we come to our conclusions.

II. QUANTUM CALCULATION

In this section, we consider a system consisting of a normal conducting waveguide of width W in contact with a semi-infinite superconducting region. We derive a secular equation. The solutions of this equation give the eigenenergies of the bound states of the system.

The eigenstates and eigenenergies can be obtained from the BdG equation,

$$\begin{pmatrix} H_0 & \Delta \\ \Delta^* & -H_0^* \end{pmatrix} \mathbf{\Psi}(x,y) = E\mathbf{\Psi}(x,y), \tag{1}$$

where $\mathbf{\Psi}$ is a two-component wave function and $H_0=(\mathbf{p}-e\mathbf{A})^2/(2m)+V-E_F$ is the single-electron Hamiltonian (for simplicity, we assume that the effective mass m and the Fermi energy E_F is the same in the N and S regions[24]). The excitation energy E is measured relative to E_F. Scattering at the NS interface is modeled by an external potential $V(x)=U_0\delta(x)$. Hard wall boundary condition is imposed at the wall of the waveguide, which is not adjacent to the superconductor, i.e., $\mathbf{\Psi}(x=W,y)=0$. The bound state energies are the positive eigenvalues $0<E<\Delta$ of the BdG equation.[19] The superconducting pair potential Δ can be approximated by a step function $\Delta(\mathbf{r})=\Delta_0\Theta(-x)$ without changing the results in any qualitative way.[25] Owing to the translational symmetry along the y direction, it is convenient to choose the Landau gauge for the vector potential: $\mathbf{A}(\mathbf{r})=B(0,x,0)^T$ (here, T denotes the transpose of a vector). The system is separable and the wave function $\mathbf{\Psi}(x,y)=[\mathbf{\Psi}_e(x,y),\mathbf{\Psi}_h(x,y)]^T$ in the N region reads

$$\mathbf{\Psi}^{(\mathbf{N})}(x,y) = \begin{pmatrix} A_e\Phi_e^{(N)}(x) \\ A_h\Phi_h^{(N)}(x) \end{pmatrix} e^{iky}, \tag{2}$$

where k is the wave number along the y direction and the amplitudes $A_{e,h}$ will be determined from the boundary conditions given below. On substituting $\mathbf{\Psi}^{(\mathbf{N})}(x,y)$ into Eq. (1), we find that the function $\Phi_e^N(x)$ satisfies the following one-dimensional Schrödinger equation,

$$\frac{d^2\Phi_e^{(N)}(\xi)}{d\xi^2} - \left(\frac{1}{4}\xi^2 + a\right)\Phi_e^{(N)}(\xi) = 0, \tag{3a}$$

where

$$\xi = \sqrt{2}\left[\frac{x}{l} - \mathrm{sign}(eB)kl\right], \quad a = -\left(\frac{E}{\hbar\omega_c} + \frac{\nu_0}{2}\right). \tag{3b}$$

Here, $l=\sqrt{\hbar/|eB|}$ is the magnetic length, $\omega_c=|eB|/m$ is the cyclotron frequency, and $\nu_0=2E_F/(\hbar\omega_c)$ is the filling factor. Equation (3a) is a parabolic cylinder differential equation.[27] The solutions, taking into account the Dirichlet boundary condition at $x=W$, can be expressed in terms of the Whittaker functions $U(a,\xi)$ and $V(a,\xi)$,

$$\Phi_e^{(N)}(x) = U(a,\xi) - \frac{U(a,\xi_W)}{V(a,\xi_W)}V(a,\xi), \tag{4}$$

where $\xi_W=\sqrt{2}[W/l-\mathrm{sign}(eB)kl]$. It follows then from the BdG equation that for the hole component $\Phi_h^{(N)}(x)$ of the wave function, the symmetry relation,

$$\Phi_h^{(N)}(B,E,x) = \Phi_e^{(N)}(-B,-E,x), \tag{5}$$

holds.

The magnetic field is assumed to be screened from the superconducting region; hence, the vector potential is taken to be zero (for the case of finite magnetic penetration length, see, e.g., Ref. 13). Therefore, in the S region, the wave function ansatz with eigenenergy E can be written as[20]

$$\mathbf{\Psi}^{(\mathbf{S})}(x,y) = \left[C_e\begin{pmatrix}\gamma_e \\ 1\end{pmatrix}\Phi_e^{(S)}(x) + C_h\begin{pmatrix}\gamma_h \\ 1\end{pmatrix}\Phi_h^{(S)}(x)\right]e^{iky}, \tag{6a}$$

where

$$\Phi_{e,h}^{(S)}(x) = e^{\pm iq_{e,h}x}, \tag{6b}$$

$$q_{e,h} = k_F\sqrt{1 - \frac{k^2}{k_F^2} \mp i\eta}, \tag{6c}$$

$\eta=\sqrt{\Delta_0^2-E^2}/E_F$, $\gamma_{e,h}=\frac{\Delta_0}{E\pm i\sqrt{\Delta_0^2-E^2}}$, and $k_F=\sqrt{2mE_F}/\hbar$ is the Fermi wave number (the upper/lower signs in the expressions correspond to the electron/hole component). Note that

in the S region, the wave function $\Psi^{(S)}(x,y)$ goes to zero for $x \to -\infty$.

The four coefficients $A_{e,h}, C_{e,h}$ in Eqs. (2) and (6a) are determined by the boundary conditions at the NS interface,[20,21]

$$\Psi^{(N)}|_{x=0} = \Psi^{(S)}|_{x=0},$$

$$\frac{d}{dx}[\Psi^{(N)} - \Psi^{(S)}]\Big|_{x=0} = \frac{2m}{\hbar^2}U_0\Psi^{(N)}\Big|_{x=0}, \tag{7}$$

for all y and k. The matching conditions shown in Eq. (7) yield a secular equation for the eigenvalues E as a function of the wave number k. Using the symmetry relations between the electronlike and holelike components of the BdG eigenspinor given by Eq. (5), the secular equation can be reduced to[20,21]

$$\mathrm{Im}\{\gamma_e D_e(E,B) D_h(E,B)\} = 0, \tag{8a}$$

where the 2×2 determinants D_e and D_h are given by

$$D_e(E,B) = \begin{vmatrix} \Phi_e^{(N)} & \Phi_e^{(S)} \\ [\Phi_e^{(N)}]' & Z\Phi_e^{(S)} + [\Phi_e^{(S)}]' \end{vmatrix}, \tag{8b}$$

$$D_h(E,B) = D_e(-E,-B). \tag{8c}$$

Here, $Z=(2m/\hbar^2)U_0$ is the normalized barrier strength, and the prime denotes the derivative with respect to x. All functions are evaluated at the NS interface, i.e., at $x=0$. The secular equation derived above is exact in the sense that the usual Andreev approximation is not assumed.[28] An analogous result was found previously[20,21] for NS disk systems.

III. SEMICLASSICAL APPROXIMATION

As a first step to calculate the conductance between the injector and the collector, we should solve the exact quantization condition [Eqs. (8)] which involves the evaluation of parabolic cylinder functions. It turns out that for certain parameter ranges, this makes the actual numerical calculations rather difficult. However, as we are going to show it in Sec. IV, for the quasiparticle dispersion relations which will be important in the subsequent analysis, one can obtain excellent approximations using semiclassical methods. The use of the semiclassical approximations makes the numerical calculations much simpler and gives a better understanding of the underlying physics. The semiclassical calculations are based on (i) the Wentzel-Kramer-Brillouin (WKB) approximation[29] of the functions $\Phi_e(x)$, $\Phi_h(x)$ [see Eqs. (3a) and (5)] and their derivatives and (ii) the Andreev approximation.[28] The approximated wave functions are then substituted into Eq. (8a) to obtain the semiclassical quantization conditions. The calculations can be carried out in a similar fashion as in Ref. 21; therefore, in this section and in the next one, we only summarize the main results. Throughout the rest of the paper, we assume an ideal NS interface, i.e., we set $U_0=0$.

Depending on the energy of the electrons (holes) and on the applied magnetic field, eight different types of orbits can be distinguished. These orbits, denoted by A to H, are shown in Fig. 2. In the geometrical construction of the classical trajectories, we took into account that the chiralities of the electronlike and the holelike orbits are preserved when electron-hole conversion occurs at the NS interface.[13]

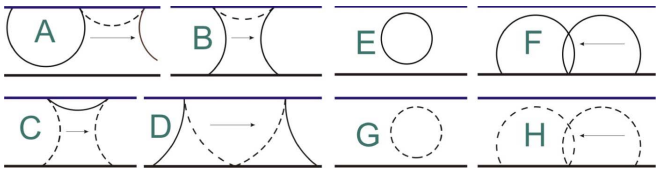

FIG. 2. (Color online) Classification of the possible orbits. The solid (dashed) lines correspond to electron (hole) trajectory segments. The black arrows show the direction of the group velocity (cf. the slope of the dispersion curves in Figs. 3 and 4) for a magnetic field pointing out of the plane.

Type A orbits correspond to the skipping motion of alternating electron and hole quasiparticles along the NS interface. Neither the trajectory of the electrons nor of the holes hits the wall of the waveguide at $x=W$. This type of orbit was first considered by Hoppe *et al.*[8] Type B and C orbits are similar to type A but either the electron or the hole can now reach the wall of the waveguide at $x=W$. In the case of type D orbits, the electrons and holes bounce both at the wall of the waveguide and at the NS interface, while for type E (G) orbits the quasiparticles move on cyclotron orbits. Type F (H) is the familiar edge state of the integer quantum-Hall systems. The electrons (holes) move on skipping orbits along the wall of the waveguide at $x=W$.

The semiclassical quantization condition for the orbits shown in Fig. 2 can be written in the following simple form:

$$N(E) = n + \mu \quad \text{for } n \in \mathbb{Z}, \tag{9a}$$

where $N(E)$ can be expressed in terms of the (dimensionless) classical action integrals $S_e(\tau_+^e, \tau_-^e)$, $S_h(\tau_+^h, \tau_-^h)$ (see Table I) of the different types of orbits and μ is the corresponding Maslov index. The actions $S_{e,h}$ are given by the following equations:

$$S_e(\tau_+^e, \tau_-^e) = 2[\Theta_e(\tau_+^e) - \Theta_e(\tau_-^e)], \tag{9b}$$

$$S_h = S_e(-E-B), \tag{9c}$$

$$\Theta_e(x) = \frac{|eB|}{2\pi\hbar}\int \sqrt{R_e^2 - (x-X)^2}\,dx = \frac{E+E_F}{2\pi\hbar\omega_c}\left[\arcsin\frac{x-X}{R_e} + \frac{1}{2}\sin\left(2\arcsin\frac{x-X}{R_e}\right)\right], \tag{9d}$$

$$\Theta_h = \Theta_e(-E,-B). \tag{9e}$$

Here, the cyclotron radii $R_{e,h}$ and the classical turning points $\tau_\pm^{e,h}$ for electrons and holes are given by

$$R_{e,h} = R_c\sqrt{1 \pm E/E_F}, \quad R_c = k_F l^2, \tag{9f}$$

$$\tau_+^e = \min\{W, X + R_e\}, \tag{9g}$$

TABLE I. $N(E)$ related to the actions defined in Eqs. (9) and the conditions for the possible types of orbits shown in Fig 2.

Type of orbit	$N(E)$	μ	Conditions for orbits
A	$S_e(\tau_+^e,\tau_-^e)-S_h(\tau_+^h,\tau_-^h)$	$\frac{1}{\pi}\arccos\left(\frac{E}{\Delta}\right)$	$\tau_+^e,\tau_+^h<W,\ \tau_-^e,\tau_-^h=0$
B	$S_e(\tau_+^e,\tau_-^e)-S_h(\tau_+^h,\tau_-^h)$	$-\frac{3}{4}+\frac{1}{\pi}\arccos\left(\frac{E}{\Delta}\right)$	$\tau_+^e=W,\ \tau_+^h<W,\ \tau_-^e,\tau_-^h=0$
C	$S_e(\tau_+^e,\tau_-^e)-S_h(\tau_+^h,\tau_-^h)$	$-\frac{1}{4}+\frac{1}{\pi}\arccos\left(\frac{E}{\Delta}\right)$	$\tau_+^e<W,\ \tau_+^h=W,\ \tau_-^e,\tau_-^h=0$
D	$S_e(\tau_+^e,\tau_-^e)-S_h(\tau_+^h,\tau_-^h)$	$\frac{1}{\pi}\arccos\left(\frac{E}{\Delta}\right)$	$\tau_+^e,\tau_+^h=W,\ \tau_-^e,\tau_-^h=0$
E	$S_e(\tau_+^e,\tau_-^e)$	$\frac{1}{2}$	$\tau_+^e<W,\ \tau_-^e>0$
F	$S_e(\tau_+^e,\tau_-^e)$	$-\frac{1}{4}$	$\tau_+^e=W,\ \tau_-^e>0$
G	$-S_h(\tau_+^h,\tau_-^h)$	$-\frac{1}{2}$	$\tau_+^h<W,\ \tau_-^h>0$
H	$-S_h(\tau_+^h,\tau_-^h)$	$-\frac{3}{4}$	$\tau_+^h=W,\ \tau_-^h>0$

$$\tau_-^e = \max\{0, X - R_e\}, \tag{9h}$$

$$\tau_\pm^h = \tau_\pm^e(-B,-E), \tag{9i}$$

where $X=\mathrm{sign}(eB)kl^2$ is the guiding center coordinate. We note that contributions to the Maslov index of a given type of orbit come from the collisions with the wall of the waveguide, from the collisions with the superconductor (Andreev reflections), and from the caustics of the electron (hole) segments of the orbit (see Table I).

IV. DISPERSION RELATION AND THE PHASE DIAGRAM FOR NS SYSTEMS

In this section, we compare the numerical results obtained from the exact quantum mechanical and from the semiclassical calculations outlined in Secs. II and III. The above discussed classical orbits can exist in different parameter ranges, depending on the strength of the magnetic field, on the Fermi energy, and on the width of the normal lead. It is convenient to use the following dimensionless parameters: ν_0, $\Delta_0/\hbar\omega_c$, k_FW, and R_c/W. Figures 3 and 4 show comparisons of the exact quantum calculations with the semiclassical results for the dispersion relation of the quasiparticles. In the case of Fig. 3, the magnetic field is strong enough so that the cyclotron radius is smaller than the width of the waveguide. One expects therefore that type A orbits and Landau levels (corresponding to orbits of types E and G) would appear in the spectrum. One can see that this is exactly the case, the Landau levels appearing as dispersionless states. The agreement between the quantum and semiclassical calculations is excellent except in the transition regime between type A and type E (G) orbits. In the case of Fig. 4, the magnetic field is weaker than for Fig. 3 and therefore R_c is now larger than W. No Landau level appears and the dispersion relation can be well approximated semiclassically using orbits of types B, C, D, F, and H.

Whether or not a given type of classical orbit is allowed for a certain set of parameter values depends on the positions of the turning points with regard to the wall of the waveguide and to the NS interface. The conditions for each type of orbits are summarized in Table I. The turning points depend

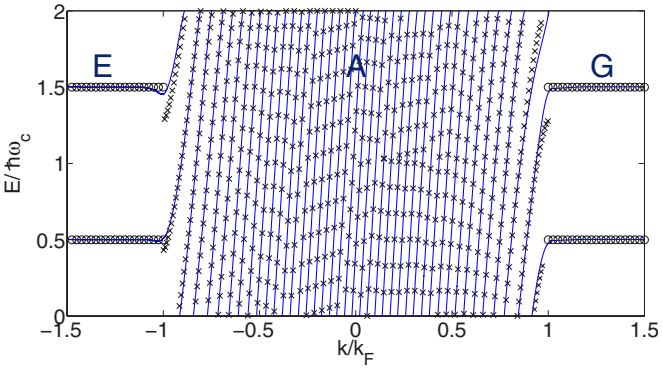

FIG. 3. (Color online) The energy spectrum obtained from Eqs. (8) (solid line) as a function of k. The parameters are $\nu_0=40$, $\Delta_0/\hbar\omega_c=2$, $k_FW=106.7$, and $R_c/W=0.375$. In the semiclassical calculations [see Eqs. (9)], only orbits of types A (×) and E and G (○) need to be taken into account.

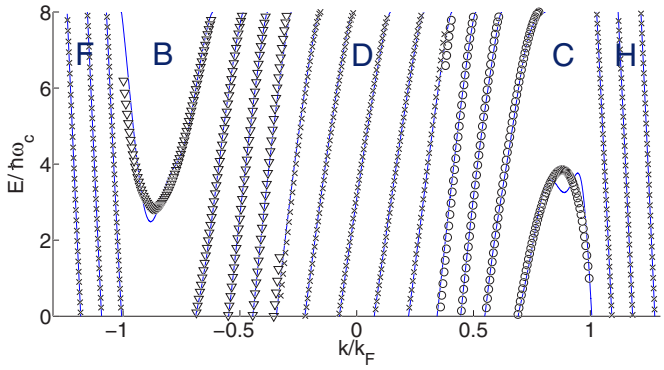

FIG. 4. (Color online) The energy spectrum obtained from Eqs. (8) (solid line) as a function of k for parameters $\nu_0=160$, $\Delta_0/\hbar\omega_c=8$, $k_FW=106.7$, and $R_c/W=1.5$. In the semiclassical calculations [see Eqs. (9)], orbits of types D, F, H (×), B (▽), and C (○) are involved.

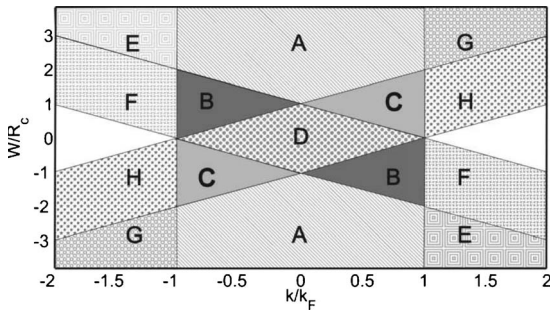

FIG. 5. The phase diagram of the allowed type of orbits as a function of R_c and k for energy $E=0$. The white regions are classically forbidden. Positive values of W/R_c correspond to magnetic field pointing out of the plane of the system, and negative W/R_c corresponds to magnetic field in the opposite direction.

[see Eqs. (9f)–(9i)] on the width of the lead W, on the Fermi wave number k_F, on the magnetic field (or equivalently, on the cyclotron radius R_c), and on the wave number k. In an experiment, the former two parameters would be fixed, R_c could be varied by varying the magnetic field, while the wave number k of the injected electrons would be uniformly distributed if there are many open channels in the quantum point contact. For a given W and k_F, i.e., for a given experimental sample, one can then draw a "phase diagram," which shows the allowed types of classical orbits as a function of R_c and k. An example of such a diagram is shown in Fig. 5. Note that the weak energy dependence of the turning points translates into a similarly weak energy dependence of the phase diagram. Thus, for Fig. 5, we have chosen $E=0$. For parameter values in the white region, no classical orbits exist.

V. COHERENT ELECTRON-HOLE FOCUSING

Having obtained the spectrum of the quasiparticles, we have now all the necessary information to calculate the conductance between the injector and the collector for the NS system shown in Fig. 1. For W_i, $W_c \ll \lambda_F$, the calculations in principle could be carried out using the exact results of Sec. II. However, this would involve evaluations of the Whittaker functions [see Eq. (4)] and we have found that this would render the actual numerical calculations rather difficult. Therefore, we calculate the conductance semiclassically, adopting and generalizing the method of Ref. 17 to account for all types of current-carrying modes. Namely, the dynamics of hole-type quasiparticles created by Andreev reflections also needs to be taken into consideration. We assume that W_i, $W_c \ll R_c$, meaning that the angular distribution of the injected electrons is not perturbed by the magnetic field.

In a classical picture, electrons having orbits of type B or D can contribute to the conductance since only these orbits reach the collector (note that for type F orbits, the group velocity points in the $-y$ direction). Assuming that the wave function in the waveguide is unperturbed by the presence of the collector,[17] the current at the collector is given by

$$I_c = \varepsilon \left[\left| \frac{\partial \Psi_e}{\partial x}(W,L) \right|^2 - \left| \frac{\partial \Psi_h}{\partial x}(W,L) \right|^2 \right], \tag{10}$$

where ε is a yet undetermined parameter but will drop out when we calculate the conductance. This expression is a generalization of Eq. (16) of Ref. 17 since it includes the contribution of the holes as well. In the WKB approximation, the wave function $\Psi^{(N)}(x,y)=[\Psi_e(x,y),\Psi_h(x,y)]^T$ in the waveguide is the sum over all classical trajectories from the injector to the point (x,y) of an amplitude factor times a phase factor. As in Ref. 17, one can transform the sum over trajectories into a sum over modes using saddle point integration. Finally, we find

$$\frac{\partial \Psi_e}{\partial x}(W,L) = -2ik_F \sum_{\substack{n \\ K=B,D}} \sqrt{2\pi i \left[\frac{\partial^2 S_e^K(p_n)}{\partial p_n^2} \right]^{-1}} A_{p_n}^K e^{ik_n^K L - i\pi} \cos \alpha_n^K \tag{11a}$$

and

$$\frac{\partial \Psi_h}{\partial x}(W,L) = -2ik_F \sum_{n} \sqrt{2\pi i \left[\frac{\partial^2 S_h^D(p_n)}{\partial p_n^2} \right]^{-1}} A_{p_n}^D e^{ik_n^D L - i\pi} \cos \alpha_n^D. \tag{11b}$$

For simplicity, here we give the definitions of the different terms appearing in the above expressions only for electrons having type B orbits. For holes and for type D orbits, similar expressions were derived but are not presented here. The wave numbers k_n of the excited modes (for a given magnetic field) can be obtained from the dispersion relation by solving the equation $E(k_n,R_c)=E$. The amplitudes $A_{p_n}^B$ of the modes related to type B orbits are given by

$$A_{p_n}^B = \sqrt{\frac{I_i \cos \alpha_n}{2v_F L} \frac{d(\alpha_n)}{d'(\alpha)|_{\alpha=\alpha_n}}}, \tag{12}$$

where I_i is the current injected from the injector, $v_F = \hbar k_F/m$ is the Fermi velocity of the quasiparticles, and the prime denotes derivation with respect to α. Here α, α_n, and $d(\alpha_n)$ are defined in the following way: the distance between two subsequent rebounds off the wall of the waveguide for an electron injected at angle α (measured from the y axis) is $d(\alpha)=4\sqrt{R_c^2-(W-R_c \sin \alpha)^2}-2R_c \cos \alpha$. Then, $p=L/d(\alpha)$ is the number of bounces between the injector and the collector. The angle α can also be expressed by $\sin \alpha=(W-X)/R_c$ and it is related to the wave number k_n of the modes. Namely, for mode k_n, the guiding center coordinate is $X=\text{sign}(eB)k_n l^2$; therefore, $\sin \alpha_n = W/R_c - \text{sign}(eB)k_n/k_F$ (because $R_c=k_F l^2$), from which it follows that $p_n=L/d(\alpha_n)$. Finally, $S_{e,(h)}^B(p_n)$ is related to the action of electrons (holes) between the injector and the collector. In the case of type B orbits, the summation over n includes only those modes for which the group velocity $\partial E(k)/\partial(\hbar k)$ is positive, i.e., the mode propagates from the injector to the collector. (Note that the group velocity is determined by the slope of the curves in Fig. 4.)

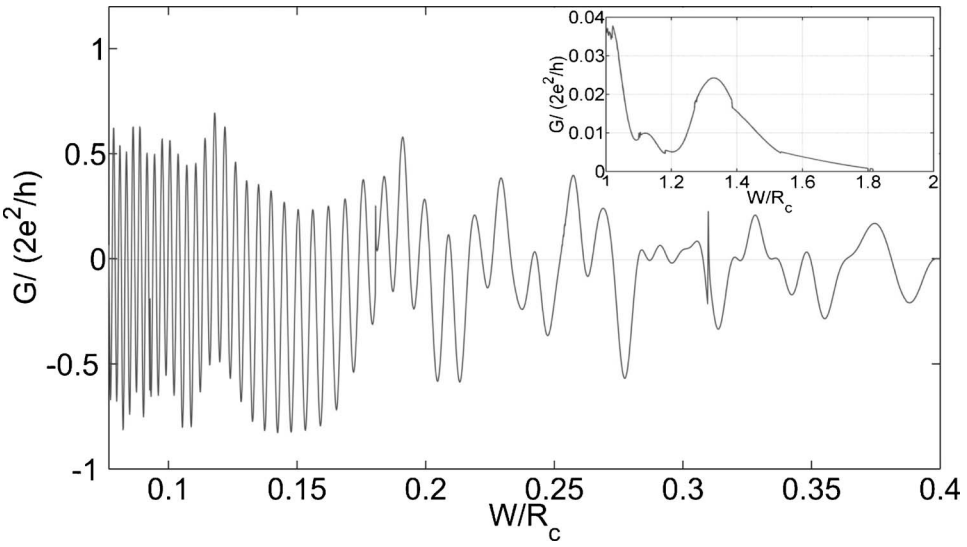

FIG. 6. The conductance G for low magnetic fields at $E=0$. Inset: the conductance for stronger magnetic fields. We used $k_F W=26.7$ and $\Delta_0/E_F=0.1$.

The conductance $G(E,R_c)$ between the injector and the collector is $G=I_i/V_c$, where V_c is the collector voltage. Taking into account Eq. (10) it reads:[17]

$$V_c = \varepsilon \left[\frac{\left| \frac{\partial \Psi_e}{\partial x}(W,L) \right|^2}{G_e} - \frac{\left| \frac{\partial \Psi_h}{\partial x}(W,L) \right|^2}{G_h} \right]. \qquad (13)$$

Here, G_e (G_h) is the conductance of the collector for electrons (holes). An estimate for G_e (G_h) is given by Eq. (17) of Ref. 17. Since both G_e and G_h are proportional to the parameter ε, it drops out from V_c. Similarly, the injected current I_i drops out from $G(E,R_c)$ since the derivatives of the wave functions in Eqs. (11) are proportional to $\sqrt{I_i}$ through the amplitudes A_{p_n}.

Equations (10), (11), and (13) allow us to calculate semiclassically the conductance as a function of the energy of quasiparticles and of the magnetic field. This is the main result of our paper. An example is shown in Fig. 6. One can clearly see that for weak magnetic fields ($W/R_c<0.4$), the conductance is a rapidly oscillating function of the magnetic field and can also take on negative values. The first observation is a consequence of the constructive interference of many coherently excited modes (edge states). A similar effect was found by van Houten *et al.*[17,18] The negative conductance values can be explained by the holelike excitations of the NS system. Indeed, at low magnetic fields (large R_c), an injected electron undergoes one or more Andreev reflections and it can happen (see type D orbits) that a hole arrives to the collector resulting in negative conductance. This is the so-called *Andreev-drag effect*.[22] In our calculations, the heights of the positive peaks are comparable to those of the negative ones. This observation is in line with the findings of Ref. 2 and also with the results of Ref. 22, where an exact (numerical) quantum calculation has been performed for the same system. We note that in the limit of $R_c/W \gg 1$, i.e., for weak magnetic fields, the conductance is to good approximation periodic in the inverse of the magnetic field $1/B$. In this limit, only type D orbits can carry current (see Fig. 5). It turns out that for certain magnetic fields, an injected flux tube of type D orbits can be focused into the collector, leading to negative or positive peaks in the conductance. The condition on the focusing magnetic fields can be cast into $R_c \approx pW^2/L$, where $p \gg 1$ is an integer. Even integers lead to positive peaks, and odd integers to negative ones in the conductance.

The use of WKB approximation implies that our results should be accurate at low magnetic fields when a large number of edge states are populated. We find, moreover, that our semiclassics predicts correctly that the conductance vanishes for strong magnetic fields in this setup (cf. Fig. 2 in Ref. 22). From the inset of Fig. 6, one can see that increasing the magnetic field, the conductance decreases and rapidly goes to zero for $W/R_c > 1.5$. This can be understood from classical considerations. Upon increasing the magnetic field, the cyclotron radius decreases and at a certain value of the field the diameter of the cyclotron orbit becomes smaller than the width of the waveguide ($W/R_c > 2$), which means that no injected electron can hit the superconductor and undergo Andreev reflections. Instead, the electrons move to the left skipping along the wall of the waveguide (type F orbits) and eventually they leave the system without reaching the collector, i.e., the conductance becomes zero. According to our semiclassical calculations, for $k_F W=26.7$ as in the case of Fig. 6, the last current-carrying mode disappears when $W/R_c \gtrsim 1.8$, in broad agreement with the classical picture.

VI. CONCLUSIONS

In conclusion, we have studied the transverse electron-hole focusing effect in a normal-superconductor system similar to the setup of Ref. 2. As a first step to determine the conductance, we calculated the energies of the bound states both quantum mechanically and in semiclassical approxima-

tion. We have shown that semiclassical methods can reproduce the results of the relevant quantum calculations and thus can help to understand the underlying physics. We have identified those classical orbits which contribute to the conductance and derived a semiclassical conductance formula. In agreement with the quantum calculations of Ref. 22, for weak magnetic fields the semiclassical conductance shows rapid oscillations and the presence of the Andreev-drag effect. For stronger magnetic fields, the conductance goes to zero, which can be understood by invoking the classical dynamics of electrons at such fields. Our results can be considered a generalization of similar works[17,18] for normal systems since in the system that we studied, the current-carrying modes are comprised of both electronlike and holelike quasiparticles. In our work, we assumed an ideal normal-superconductor interface, i.e., neglected the probability of specular reflection. Given the interface quality that can be achieved with present-day fabrication techniques, an important extension of the present work would be to consider both quantum mechanically and semiclassically the effects of a finite interface barrier ($U_0 \neq 0$) and mismatch in the Fermi velocities and effective masses.

ACKNOWLEDGMENT

This work is supported by European Commission Contract No. MRTN-CT-2003-504574.

[1] A. F. Morpurgo, B. J. van Wees, T. M. Klapwijk, and G. Borghs, Phys. Rev. Lett. **79**, 4010 (1997); R. J. Soulen, Jr., J. M. Byers, M. S. Osofsky, B. Nadgorny, T. Ambrose, S. F. Cheng, P. R. Broussard, C. T. Tanaka, J. Nowak, J. S. Moodera, A. Barry, and J. M. D. Coey, Science **282**, 85 (1998); V. A. Vasko, V. A. Larkin, P. A. Kraus, K. R. Nikolaev, D. E. Grupp, C. A. Nordman, and A. M. Goldman, Phys. Rev. Lett. **78**, 1134 (1997); M. Giroud, H. Courtois, K. Hasselbach, D. Mailly, and B. Pannetier, Phys. Rev. B **58**, R11872 (1998); S. K. Upadhyay, R. N. Louie, and R. A. Buhrman, Appl. Phys. Lett. **74**, 3881 (1999); V. T. Petrashov, I. A. Sosnin, I. Cox, A. Parsons, and C. Troadec, Phys. Rev. Lett. **83**, 3281 (1999); M. D. Lawrence and N. Giordano, J. Phys.: Condens. Matter **11**, 1089 (1999); F. J. Jedema, B. J. van Wees, B. H. Hoving, A. T. Filip, and T. M. Klapwijk, Phys. Rev. B **60**, 16549 (1999); J. Eroms, M. Tolkiehn, D. Weiss, U. Rössler, J. DeBoeck, and S. Borghs, Europhys. Lett. **58**, 569 (2002); B.-R. Choi, A. E. Hansen, T. Kontos, C. Hoffmann, S. Oberholzer, W. Belzig, C. Schönenberger, T. Akazaki, and H. Takayanagi, Phys. Rev. B **72**, 024501 (2005); S. Russo, M. Kroug, T. M. Klapwijk, and A. F. Morpurgo, Phys. Rev. Lett. **95**, 027002 (2005).

[2] P. A. M. Benistant, H. van Kempen, and P. Wyder, Phys. Rev. Lett. **51**, 817 (1983).

[3] P. A. M. Benistant, A. P. van Gelder, H. van Kempen, and P. Wyder, Phys. Rev. B **32**, 3351 (1985).

[4] T. D. Moore and D. A. Williams, Phys. Rev. B **59**, 7308 (1999); T. Akazaki, H. Yamaguchi, J. Nitta, and H. Takayanagi, Supercond. Sci. Technol. **12**, 901 (1999).

[5] J. Eroms, D. Weiss, J. De Boeck, G. Borghs, and U. Zülicke, Phys. Rev. Lett. **95**, 107001 (2005).

[6] I. E. Batov, Th. Schapers, N. M. Chtchelkatchev, H. Hardtdegen, and A. V. Ustinov, arXiv:0704.3017v2 (unpublished).

[7] Y. Takagaki, Phys. Rev. B **57**, 4009 (1998); Y. Asano, *ibid.* **61**, 1732 (2000).

[8] H. Hoppe, U. Zülicke, and G. Schön, Phys. Rev. Lett. **84**, 1804 (2000).

[9] N. M. Chtchelkatchev, JETP Lett. **73**, 94 (2001).

[10] M. Schechter, Y. Imry, and Y. Levinson, Phys. Rev. B **64**, 224513 (2001).

[11] N. G. Fytas, F. K. Diakonos, P. Schmelcher, M. Scheid, A. Lassl, K. Richter, and G. Fagas, Phys. Rev. B **72**, 085336 (2005).

[12] G. Fagas, G. Tkachov, A. Pfund, and K. Richter, Phys. Rev. B **71**, 224510 (2005).

[13] F. Giazotto, M. Governale, U. Zülicke, and F. Beltram, Phys. Rev. B **72**, 054518 (2005).

[14] N. M. Chtchelkatchev and I. S. Burmistrov, Phys. Rev. B **75**, 214510 (2007).

[15] A. F. Andreev, Zh. Eksp. Teor. Fiz. **46**, 1823 (1964) [Sov. Phys. JETP **19**, 1228 (1964)].

[16] V. S. Tsoi, J. Bass, and P. Wyder, Rev. Mod. Phys. **71**, 1641 (1999).

[17] H. van Houten *et al.*, Phys. Rev. B **39**, 8556 (1989).

[18] H. van Houten and C. W. J. Beenakker, in *Analogies in Optics and Micro Electronics*, edited by W. van Haeringen and D. Lenstra (Kluwer, Dordrecht, 1990); arXiv:cond-mat/0512611v1 (unpublished).

[19] P. G. de Gennes, *Superconductivity of Metals and Alloys* (Benjamin, New York, 1996).

[20] J. Cserti, A. Bodor, J. Koltai, and G. Vattay, Phys. Rev. B **66**, 064528 (2002).

[21] J. Cserti, P. Polinák, G. Palla, U. Zülicke, and C. J. Lambert, Phys. Rev. B **69**, 134514 (2004).

[22] P. K. Polinák, C. J. Lambert, J. Koltai, and J. Cserti, Phys. Rev. B **74**, 132508 (2006).

[23] S. Sanvito, C. J. Lambert, J. H. Jefferson, and A. M. Bratkovsky, Phys. Rev. B **59**, 11936 (1999).

[24] For different effective masses see, for example, Refs. 20 and 21.

[25] C. W. J. Beenakker, Lect. Notes Phys. **667**, 131 (2005).

[26] C. J. Lambert and R. Raimondi, J. Phys.: Condens. Matter **10**, 901 (1998).

[27] A. Abramowitz and I. A. Stegun, *Handbook of Mathematical Functions* (Dover, New York, 1972).

[28] In Andreev approximation, making use of the fact that usually $\Delta_0/E_F \ll 1$ and assuming that the quasiparticles are incident at the NS interface almost perpendicularly, one neglects the normal reflection. See, e.g., Ref. 26.

[29] M. Brack and R. K. Bhaduri, *Semiclassical Physics*, edited by D. Pines (Addison-Wesley, Amsterdam, 1997).